The Nitridation of Chromium and Cr-Ti Alloys

JERRY L. ARNOLD AND WILLIAM C. HAGEL

Reaction zones and growth kinetics were studied after exposing high-purity chromium and alloys containing 0.5, 3.0, and 5.0 wt pct Ti to 1 atm of nitrogen between 1000° and 1400°C. Outer layers of Cr_2N and regions of internal nitridation, containing dispersed TiN particles, grew in a parabolic manner. An exact solution of Maak's simplified analysis for internal oxidation provided calculations of nitrogen diffusion in the internal-nitride zone of each alloy. Extrapolation gave the relationship $D = 9.6 \times 10^{-3} \exp(-28{,}500/RT)$ cm^2 sec^{-1} for nitrogen diffusion in high-purity chromium. Increasing titanium to 5.0 wt. pct gave $D = 2.5 \times 10^{-3} \exp(-24{,}000/RT)$ cm^2 sec^{-1}.

ALTHOUGH chromium and its alloys form nitrides and embrittle from the nitrogen in hot air, little attention has been given the gas-metal reaction, known as nitridation, where nitrogen is the sole gas during high-temperature exposure. In 1962, Hagel[1] used a microbalance to follow the weight gained by iodide chromium, with and without 0.9 wt pct Y, in nitrogen at 76 mm Hg between 650° and 1000°C. A Cr_2N layer grew inward at a parabolic rate on the surface, and no internal nitrides were observed. Seybolt and Haman[2] stated that the rate of Cr_2N formation is controlled by nitrogen diffusion through Cr_2N and that this rate at 1000°C is some 30 times faster than the rate of oxidation to Cr_2O_3.

Chromium-base alloys also exhibit almost 100 times greater solubility for nitrogen than for oxygen and internal nitridation is a characteristic feature. Henderson *et al.*[3] nitrided chromium alloys with up to 2 wt pct of Ti, Ce, Al, and Ta and found low brittle-ductile transition temperatures as more stable nitrides replaced Cr_2N and apparently scavenged nitrogen from the matrix. Ryan and Johnstone[4] prepared Cr-Ti-N alloys by adding nitrogen directly to the melt and found high strengths and ductilities. However, some of the TiN particles observed were 1 to 2 μ in width, and finer sizes are desirable for effective dispersion strengthening.

The objectives of this investigation were: 1) to establish microscopically the nitridation kinetics of high-purity chromium and Cr-Ti alloys, up to 5 wt pct Ti; 2) to examine the nitrides which form and their effect on alloy hardness; 3) to provide nitrogen diffusion coefficients for this system.

THEORY

Since internal oxidation and internal nitridation are equivalent fundamentally, earlier studies of the former were utilized for working relationships. Easily adapted is Wagner's[5] analysis which can be stated as

$$\xi = 2\gamma(Dt)^{1/2} \qquad [1]$$

where ξ is the depth of the internal-nitride zone, γ is a constant at a given temperature, composition, and gas pressure, D is the diffusion coefficient for nitrogen in the internal-nitride zone, and t is exposure time. The parameter γ is solved graphically or numerically using the relationship

$$N/N_{Ti} = \exp(\gamma^2)\, erf(\gamma)/Q^{1/2} \exp(\gamma^2\varphi)\, erfc(\gamma\varphi^{1/2}) \qquad [2]$$

where N equals the mole fraction of nitrogen at the external surface, N_{Ti} equals the mole fraction of the solute element, titanium, in the bulk alloy, and φ is the ratio of D divided by D_{Ti} for diffusion of the solute element in the bulk alloy.

Maak[6] treated the situation where an external scale, such as Cr_2N, grows parabolically in addition to simple internal nitridation. Here the external-scale thickness X is described by

$$X = (2k_c t)^{1/2} \qquad [3]$$

where k_c is a normal corrosion constant. Another relationship using k_c

$$N_N/N_{Ti} = \exp(\gamma^2)[erf\,\gamma - erf(k_c/2D)^{1/2}]/Q^{1/2}$$
$$\exp(\gamma^2\varphi)\, erfc(\gamma\varphi^{1/2}) \qquad [4]$$

again provides for a solution of γ. The mole fraction N_N represents nitrogen concentration at the Cr_2N/inner-nitride interface and is equal to the solubility limit of nitrogen in pure chromium. When $\gamma \ll 1$ and $X < \xi$, Eq. [4] reduces to

$$N_N D = N_{Ti}\, \xi(\xi - X)/2tF[\xi/2(D_{Ti}t)^{1/2}] \qquad [5]$$

where the auxiliary function F is defined as

$$F(u) = \pi^{1/2} u e^{u^2}\, erfc(u) \qquad [6]$$

The value of ξ now equals total reaction zone thickness while D represents the diffusion coefficient of nitrogen through the internal-nitride zone, which is nearly pure chromium with dispersed TiN.

As the present study progressed, the assumption of $\gamma \ll 1$ was found not to apply under many test conditions and Eq. [4] had to be solved exactly. From Eq. [1], we obtained

$$D^{1/2} = (\xi/t^{1/2})/2\gamma \qquad [7]$$

Dividing Eq. [3] by Eq. [1] and rearranging yields

$$(k_c/2D)^{1/2} = \gamma[(X/t^{1/2})/(\xi/t^{1/2})] \qquad [8]$$

Since $\varphi = D/D_{Ti}$, Eq. [1] can also be expressed as

$$\gamma^2\varphi = \xi^2/4D_{Ti}t \qquad [9]$$

Substitution of these relations into Eq. [4] and rearranging gives

$$\exp(-\gamma^2)/\gamma = [erf(\gamma) - erf(\gamma X/\xi)]$$

JERRY L. ARNOLD is Research Metallurgist, Armco Steel Corporation, Middletown, Ohio. WILLIAM C. HAGEL is Manager, Materials Development, Materials and Process Technology Laboratories, Aircraft Engine Group, General Electric Co., Cincinnati, Ohio.

Manuscript submitted October 11, 1971.

$$\times [2N_{Ti}D_{Ti}^{1/2} \exp(\xi^2/4D_{Ti}t)/N_N(\xi/t^{1/2})\, erfc(\xi/4D_{Ti}t)^{1/2}] \quad [10]$$

The terms X, ξ, and t are measured experimentally for each composition, N_{Ti}, at each test temperature. Values for N_N were taken from Schwerdtfeger's[7] data for the solubility limit of nitrogen in chromium between 1000° and 1450°C; D_{Ti} values for titanium diffusion in chromium have been given by Adda and Philibert.[8] Eq. [10] is a transcendental equation solved graphically by plotting curves for both the left and right sides on the same graph as a function of γ; the intersection represents γ for that test condition. This value is then substituted into Eq. [1] along with measured ξ and t values to give D.

EXPERIMENTAL PROCEDURE

Buttons of chromiun and Cr-Ti alloys were prepared by arc-melting preweighed amounts of high-purity iodide material. The metal was melted in a water-cooled copper crucible using a nonconsumable tungsten electrode under an inert atmosphere of argon. Coring was minimized by numerous remelts and homogenizations near the melting point. Final compositions of the Cr-Ti alloys were 0.51, 3.04, and 5.05 wt pct Ti. These values can be converted to 0.55, 3.29, and 5.46 at. pct Ti, but are henceforth referred to as 0.5, 3.0, and 5.0 wt pct Ti alloys.

Cubic blocks that were approximately 5 mm on each edge were cut from the buttons, ground flat on 000 emery paper, and degreased in acetone and ethyl alcohol. They were placed in Kanthal- and platinum-wound furnaces and reacted at 1000°, 1050°, 1125°, 1200°, 1300°, or 1400°C. A monitoring Pt/Pt-13 Rh thermocouple indicated that temperatures were maintained constant to ±2°C with peak-to-peak variations on an average of once every 30 min. A continuous temperature record was maintained, and corrections for heating and cooling of specimens were applied to give equivalent time at temperature.

The nitrogen used here was initially 99.999 pct pure and was passed through Drierite and over copper turnings maintained at 600°C. Further gettering was accomplished by placing chromium chips around the specimens sitting in their zirconia reaction boats. No oxide films were seen on sample surfaces unless a reaction tube cracked. Nitrogen pressure was just about 2.5 cm of oil above atmospheric since an oil-filled bottle was used at the exit end of the nitridation chamber to follow a flow rate of 50 $cm^3\ min^{-1}$.

Each alumina reaction tube had gas entering at one end and exiting at the other. An O-ring seal was used to open the tube, and its face plate also had another O-ring seal allowing passage of a cemented alumina thermocouple rod through the middle. Attached to the inner end of the rod was a zirconia boat used to hold the specimens. Hence, a thermocouple tip was always over the specimens; the boats were inserted and removed in steps of 2.5 cm min^{-1} by motion of the thermocouple under a clean nitrogen atmosphere. A boat would contain four identified specimens of 0, 0.5, 3.0, and 5.0 wt pct Ti; these were all in the same constant temperature zone and would have the same exposure time.

Faces of the four specimens were glued with thin Duco cement to a small plate of titanium and placed in a standard-size transparent Lucite metallographic mount. The titanium plate was used to keep all specimen sides perpendicular to the direction of observation and to prevent edge rounding. The transparent mount was helpful in observing whether the specimens had shifted during mounting. The specimen cubes were sectioned and prepared by standard metallographic methods. An electrolytic etch, using 3 v in 5 pct oxalic acid for 3 to 60 sec, dramatically revealed the outer Cr_2N layer and the zone of internal nitridation. Distances were measured from the surface adjacent to the titanium plate to the innermost edge of each region.

Metallographic examinations were performed on a Reichert inverted-stage metallograph. A Filar eyepiece was calibrated with three objectives to measure a large range of thicknesses. Ten measurements were made of each X and ξ region to give reliable averages. Specimens selected for electron microscopy were replicated using 1 mil thick cellulose-acetate tape. The stripped replicas were placed in a vacuum bell jar, shadowed with platinum at 15 deg, covered with carbon at 90 deg, and attached to a 200-mesh electron-microscope grid. A Philips EM-200 electron microscope was used for further photography. Microhardness measurements of the samples were taken using a Tukon tester and a standard 135 deg diamond-pyramid indenter under a load of 0.2 kg. Scans were made perpendicular to the flat exposed surface. Nitride identifications were performed using the standard Debye-Scherrer powder-diffraction camera technique for d-spacings.

EXPERIMENTAL RESULTS

Thickness data were initially analyzed using a SCM Marchant desk calculator programmed to write each datum point and perform individual summations. Calculations of average thickness and its standard deviation were in terms of Filar units. These data along with corresponding magnifications, time, temperatures, and compositions served as the basis for input data for subsequent computer calculations.

Metallographic examination with a light microscope showed that all specimens had a single outer scale with a columnar structure of elongated grains grown perpendicular to the surface. With the Cr-Ti alloys, an internal-nitride zone was obvious beneath the Cr_2N outer scale, as shown in Fig. 1(a). This zone was composed of fine TiN particles uniformally dispersed in a matrix of chromium. The boundary between the Cr_2N and the internal nitride was always distinct, and there was no problem in determining its position; the boundary between the internal nitride and unreacted matrix was more irregular and less distinct. Accurately measuring the thickness of the internal region was not difficult because the TiN particles were easily discerned using polarized light. The outer scale of Cr_2N generally contained TiN precipitates which had been enveloped by the advancing front. However, at lower temperatures and titanium concentrations, one could see evidence of TiN going into solution into the Cr_2N.

Lower temperature tests showed evidence of some preferential TiN precipitation at subgrain boundaries, as shown in Fig. 1(b). This accelerated precipitation was probably due to the greater diffusion of nitrogen along these short-circuiting paths at lower temperatures. The effect decreased considerably at 1050°C

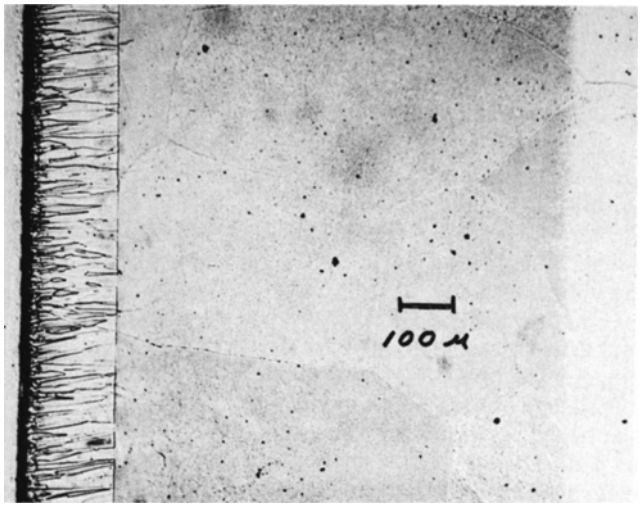

(a)

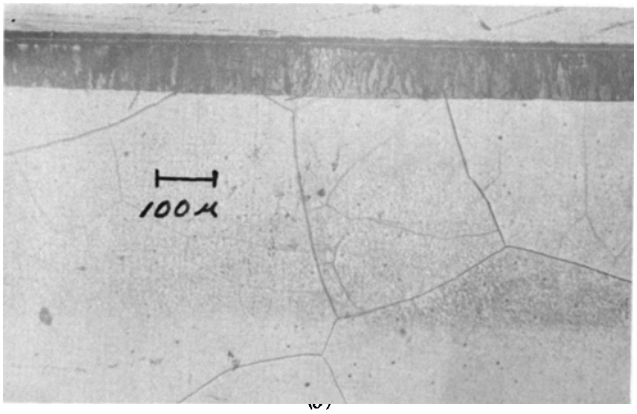

Fig. 1—(*a*) Internal-nitride zone of Cr-0.5 wt pct Ti specimen held in nitrogen for 317 min at 1200°C. (*b*) Preferential precipitation at subgrain boundaries in Cr-0.5 wt pct Ti specimen held for 1866 min at 1000°C.

and was essentially zero at 1125°C and higher.

TiN particle shape also varied with reaction temperature. At 1000°, 1050°, and 1125°C, the particles appeared to have no definite shape and approached being spherical with a diameter of about 1000Å. Particle shape became plate-like at 1200°C, and at 1400°C the particles were almost entirely in the form of 1 μ wide platelets, Fig. 2. Calculated volume percents of TiN varied from about 1 to 6 for the 0.5 to 3.0 wt pct Ti specimens, respectively, at the temperatures cited. Another metallographic observation was the occurrence of banded precipitation in the inner nitride zone, as shown in Fig. 3. Only the 3.0 and 5.0 wt pct Ti alloys showed banding, and then only at temperatures below 1125°C. The banded structure consisted of alternating high and low concentrations of TiN particles with the bands forming parallel to the external surface. Other investigators have noted similar structures resulting from internal oxidation, and Meijering and Dreuyvesteyn[9] proved that they were caused by temperature fluctuations. The number of bands roughly correponded to the frequency of thermal cycling measured in these furnaces, even though the cycling was only over a 4°C temperature range.

Microhardness profiles across the various reaction zones showed generally uniform high values in Cr_2N

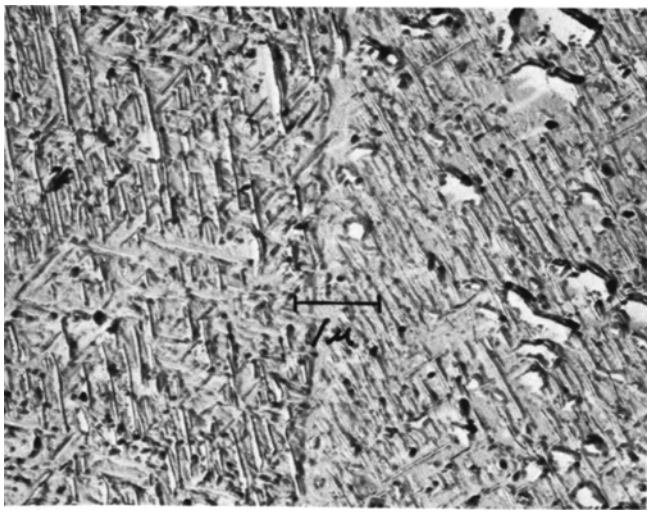

Fig. 2—Internal-nitride platelets on both sides of a grain boundary in a Cr-3.0 wt pct Ti specimen held for 40 min at 1400°C.

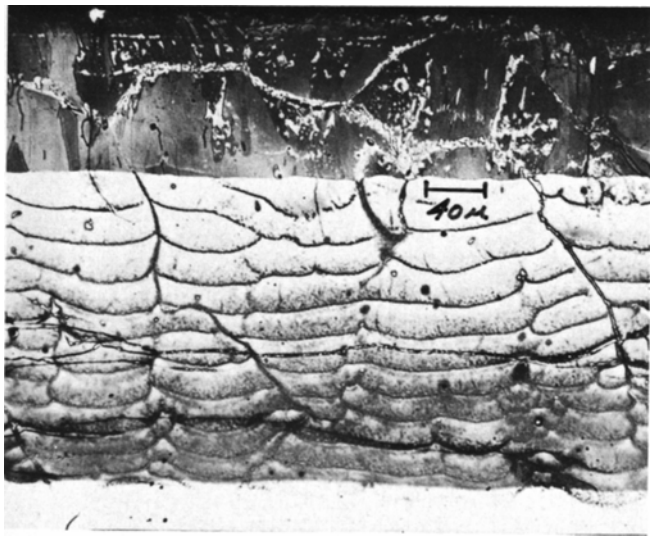

Fig. 3—Cr-3.0 wt pct Ti specimen displaying banded precipitation in the internal-nitride zone after 1600 min at 1050°C.

(Vhn $\simeq$ 1500) with inner-nitride zone values decreasing linearly to those for the unreacted matrix (Vhn $\simeq$ 250). Five measurements were taken across the internal-nitride zone and two were of the unreacted matrix. Meaningful trends could be followed by using a ratio of average hardness for the internal zone divided by matrix hardness. This ratio increased with increasing titanium concentration, *i.e.*, a greater volume percent of TiN, and with decreasing nitridation temperature, *i.e.*, smaller particle size. In fact maxima occurred as are shown in Fig. 4; these data are similar to aging curves for other precipitation-hardened alloys. At longer times, hardness falls off considerably as overaging occurs. The maximum hardness attained at each temperature decreases in a uniform manner with increasing test temperature while the time to reach this maximum also decreases. The 1050°C peak ratio of 3.89 came from an average internal-nitride Vhn equal to 1026 for a matrix hardness of 264. This is a high degree of dispersion strengthening within an internal-nitride zone that is 185 μ thick after 1050 min exposure time.

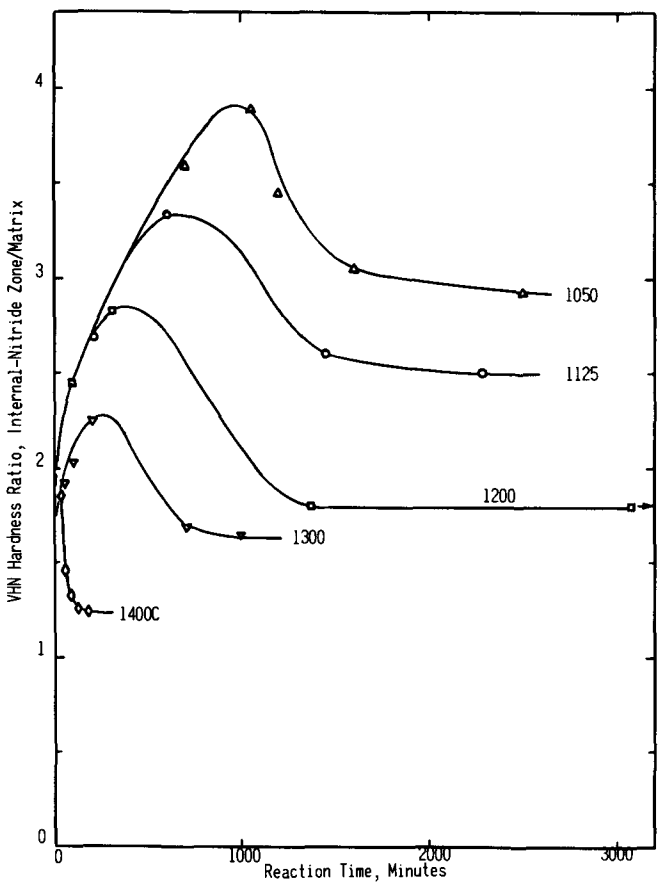

Fig. 4—Ratio for the average hardness of the internal-nitride zone divided by matrix hardness vs reaction time at various temperatures for Cr-3.0 wt pct Ti.

Thickness data for the Cr_2N layer (X) and the total nitrogen-affected zone (ξ) were squared and plotted as a function of reaction time. A high degree of linearity was observed, indicating conformance to the parabolic rate law, and a least-squares analysis was applied to give the rate constants listed in Table I. Sample plots for X^2 and ξ^2 vs time at various temperatures for the Cr-3 wt pct Ti alloy are displayed as Figs. 5 and 6.

The Cr_2N reaction-rate constants taken from the above plots and listed in Table I are equal to $2k_c$ in Eq. [3]. The Arrhenius expression showing temperature dependency is

$$k_c = k_c^\circ \exp(-E/RT) \qquad [11]$$

where k_c° is a preexponential constant, E is an activation energy for Cr_2N growth and R is the gas constant. Performing a least-squares analysis in the form of $\ln k_c$ vs $1/T$ allows one to calculate E and k_c°. These results are presented in Table II. Note that both E and k_c° decrease considerably with increasing titanium content. Conversion of k_c's to constants for parabolic weight gain, *i.e.* the more familiar gravimetric k_p values, is made by the relationship

$$k_p = 2k_c\, y^2\, \delta^2_{Cr_2N} \qquad [12]$$

where y is the wt fraction of nitrogen in Cr_2N and δ_{Cr_2N} is the density of Cr_2N. The latter numbers are taken as 0.119 and 6.63 g cm^{-3}, respectively. The parabolic weight-gain expression for Cr_2N growth on high-purity chromium is

$$k_p = 5.63 \times 10^2 \exp(-72{,}400 \pm 3300/RT)$$
$$g^2\ cm^{-4}\ sec^{-1} \qquad [13]$$

At 1000°C, $k_p = 2.03 \times 10^{-10}$ g^2 cm^{-4} sec^{-1} which is in good agreement with the 4×10^{-10} measured by Seybolt and Haman. Arkharov *et al.*[10] have studied the nitridation of chromium in ammonia and obtained a preexponential for Eq. [13] of 13.6×10^2 g^2 cm^{-4} sec^{-1} and an E of 73,600 cal per mole; this also is in good agreement, considering possible differences between the two investigations.

From known experimental values and appropriate substitutions into Eq. [10], γ's for all test conditions were determined and used in Eq. [1] for the D values listed in Table III. These were plotted in Fig. 7 with the passage of least-squares lines through each family of points. Q and D_0 results are tabulated in Table IV where it is seen that increasing titanium causes a decrease in Q and D_0. Extrapolation to zero titanium yields the expression

$$D = 0.0096 \exp(-28{,}500 \pm 2000/RT)\ cm^2\ sec^{-1} \qquad [14]$$

for nitrogen diffusion in high-purity chromium.

DISCUSSION

Results previously reported for nitrogen diffusion in chromium are listed in Table V and plotted in Fig.

Table I. Parabolic Rate Constants for Growth of Cr_2N and Internal Nitride

At. Pct Ti	Number of Data Points	Cr_2N Rate Constant, $cm^2\ sec^{-1}$	Correlation Coefficient	Number of Data Points	Internal-Nitride Rate Constant, $cm^2\ sec^{-1}$	Correlation Coefficient
1000°C						
0.0	8	2.34×10^{-10}	0.355			
0.55	5	5.97×10^{-10}	0.834	5	2.75×10^{-8}	0.994
3.29	9	6.75×10^{-10}	0.916	9	6.08×10^{-9}	0.991
5.46	5	6.57×10^{-10}	0.853	5	5.29×10^{-9}	0.996
1050°C						
0.0	5	1.42×10^{-9}	0.810			
0.55	5	1.24×10^{-9}	0.752	5	5.97×10^{-8}	0.995
3.29	10	1.60×10^{-9}	0.931	10	1.21×10^{-8}	0.977
5.46	6	1.76×10^{-9}	0.918	6	1.01×10^{-8}	0.992
1125°C						
0.0	5	5.03×10^{-9}	0.996			
0.55	5	4.39×10^{-9}	0.944	5	2.39×10^{-7}	0.996
3.29	9	5.31×10^{-9}	0.995	9	4.07×10^{-8}	0.996
5.46	5	5.93×10^{-9}	0.996	5	2.67×10^{-8}	0.997
1200°C						
0.0	5	1.61×10^{-8}	0.996			
0.55	5	1.56×10^{-8}	0.993	5	5.99×10^{-7}	0.997
3.29	7	1.22×10^{-8}	0.996	7	1.32×10^{-7}	0.999
5.46	5	1.29×10^{-8}	0.998	5	9.35×10^{-8}	1.000
1300°C						
0.0	3	7.75×10^{-8}	1.000			
0.55	4	6.18×10^{-8}	0.993	4	1.98×10^{-5}	0.978
3.29	5	5.47×10^{-8}	1.000	5	5.50×10^{-7}	0.998
5.46	4	4.45×10^{-8}	0.998	4	3.97×10^{-7}	0.999
1400°C						
0.0	7	2.94×10^{-7}	0.999			
0.55	5	2.26×10^{-7}	0.999	5	7.08×10^{-6}	0.992
3.29	5	1.90×10^{-7}	0.991	5	1.87×10^{-6}	1.000
5.46	7	1.70×10^{-7}	0.999	7	1.28×10^{-6}	0.998

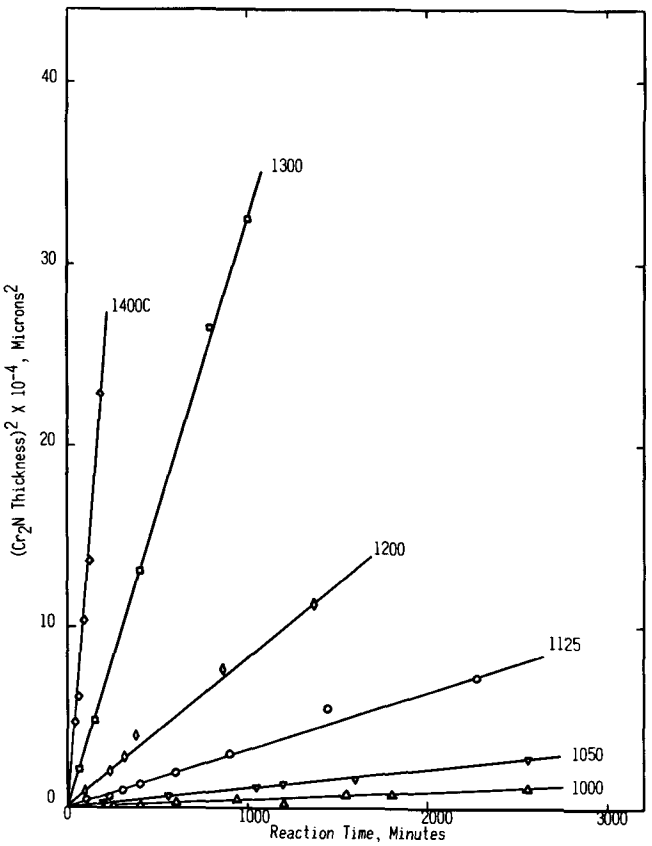

Fig. 5—Cr_2N thickness squared vs reaction time at various temperatures for Cr-3.0 wt pct Ti.

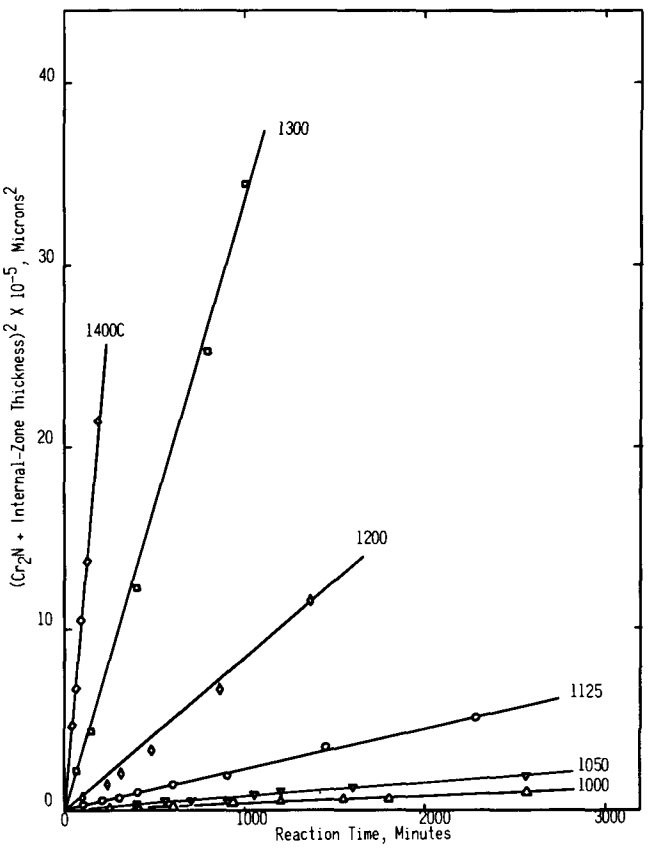

Fig. 6—Internal-nitride zone thickness squared vs reaction time at various temperatures for Cr-3.0 wt pct Ti.

8. Although differences are exaggerated by extrapolation to zero reciprocal temperature, they are fairly consistent from 50° to 1400°C. What is perhaps unexpected is that the low-temperature data up to 175°C do not show more upward curvature from short-circuit diffusion along grain boundaries or dislocations. Buck and Waterhouse[11] have reported some nitrogen segregation at subgrain boundaries and dislocations but no observable grain-boundary penetration. Volume diffusion of nitrogen appears to exceed greatly whatever form of short-circuit diffusion is also occurring, *e.g.* the subgrain boundary diffusion shown in Fig. 1(*b*).

From the reasoning of Wert and Zener,[15] one can calculate the diffusional Q in accordance with

$$Q = Ar^2T_m/1 - \beta \qquad [15]$$

where A equals 1.3×10^{17} cal mole^{-1} K^{-1} cm^{-2}, [16] r is the Goldschmidt radius of nitrogen taken as 0.71Å, β represents the temperature dependence of the shear modulus and equals 0.528,[17] and T_m is the melting temperature of chromium expressed as 2148 K. This gives a Q approximately equal to 30,000 cal mole^{-1} and tends to reinforce the 28,500 cal mole^{-1} found here for high-purity chromium. Zener's analysis[18] for calculating D_0 employs the relationship

$$D_0 = \rho\nu\ a^2 \exp(\Delta S/R) \qquad [16]$$

where ρ is a geometric constant equal to $\frac{1}{6}$ for interstitials in a bcc lattice, ν is the atomic vibration frequency in plane {100} assumed as 10^{13} sec^{-1}, a is the chromium lattice parameter or 2.88Å, and $\Delta S = Q/T_m$ or 7.05 cal mole^{-1} K^{-1}. Substitution into Eq. [16] gives a calculated D_0 of 0.049 cm^2 sec^{-1} which is also plotted as $1/T = 0$ in Fig. 8. The experimental value of 0.0096 cm^2 sec^{-1} is higher than previous studies and is not greatly lower than the calculated value when compared on a logarithmic basis. Nitrogen diffusion in bcc Ta, Fe, and Nb gives experimental D_0's of 0.0056, 0.003, and 0.0086 cm^2 sec^{-1}, respectively,[19] which are also lower than the predicted values of 0.018, 0.010, and 0.024 cm^2 sec^{-1}.

The observed minor compositional dependence displayed by the calculated diffusion coefficients might be the result of two conditions which are occurring simul-

Table II. Calculated Values Describing Growth of Cr_2N

Wt Pct Ti	0.0	0.5	3.0	5.0
E, cal mole^{-1}	72,400	63,500	59,000	56,800
Standard deviation of E	±3,300	±1,300	±1,600	±1,700
k_c^o, cm^2 sec^{-1}	455	20.9	4.35	2.01
Correlation coefficient	0.996	0.999	0.999	0.998

Table III. Diffusion Coefficients for Nitrogen in the Internal-Nitride Zone of Cr-Ti Alloys as Determined by an Exact Solution of Maak's Analysis

Temperature, °C	D, cm^2 sec^{-1}		
	0.5 Pct Ti	3.0 Pct Ti	5.0 Pct Ti
1000	1.36×10^{-7}	1.74×10^{-7}	2.51×10^{-7}
1050	1.79×10^{-7}	1.96×10^{-7}	2.58×10^{-7}
1125	3.68×10^{-7}	3.13×10^{-7}	3.04×10^{-7}
1200	5.16×10^{-7}	5.64×10^{-7}	6.25×10^{-7}
1300	9.28×10^{-7}	1.08×10^{-6}	1.27×10^{-6}
1400	2.09×10^{-6}	1.96×10^{-6}	2.05×10^{-6}

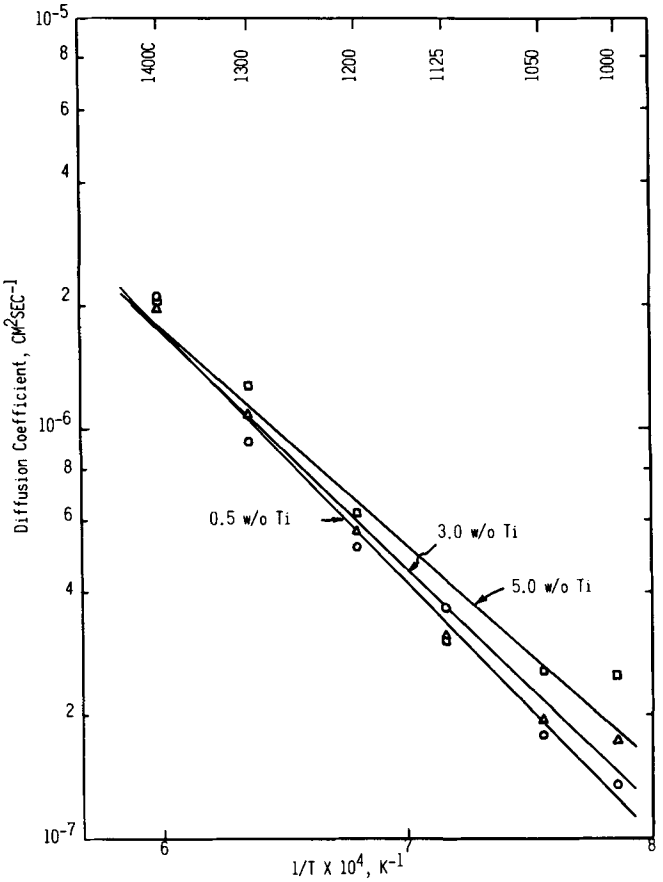

Fig. 7—Diffusion coefficients for nitrogen diffusion in Cr-Ti alloys vs reciprocal temperature.

Table IV. Results of Arrhenius Analysis of Diffusion Data

	Extrapolated 0 Pct Ti	0.5 Pct Ti	3.0 Pct Ti	5.0 Pct Ti
Q, cal mole^{-1}	28,500	28,200	26,600	24,000
Standard deviation Q	±2,000	±1,500	±1,800	±3,100
D_0, cm^2 sec^{-1}	0.0096	0.0090	0.0054	0.0025
Correlation coefficient	–	0.994	0.991	0.968

taneously. The first is the result of the nonzero volume of the internal-nitride precipitates. As titanium concentration is increased, the volume fraction of TiN would also be increased, thus reducing the effective cross-section available for nitrogen diffusion through the internal-nitride zone, while the source of nitrogen at the Cr_2N interface remains unchanged. This would be analogous to the increased velocity of a fluid through the region of a pipe with a reduced cross-section. Thus the apparent diffusion coefficient of nitrogen through the inner nitride zone would increase as titanium is increased. The second condition which might contribute to increased growth rates of both the total reaction zone and the Cr_2N thickness is that there might be a slight solubility of titanium in the Cr_2N. Seybolt and Haman[2] have shown that diffusion of nitrogen inward from the surface controls the growth of the Cr_2N scale and they also state that this is not a typical ionic scale, but one where metallic or covalent bonding predominate. Any solution of titanium into the Cr_2N lattice would be expected to increase the apparent solubility of nitrogen since each titanium atom would contribute one nitrogen atom while the original Cr_2N had only $\frac{1}{2}$ nitrogen atom per metal atom. One is increasing the number of rate-controlling atoms and higher rates of Cr_2N growth would thus be expected. Increasing the nitrogen concentration at the Cr_2N/internal nitride interface slightly would cause a greater composition gradient across the internal-nitride zone, with resultant slightly increased growth rates of this zone also. Extrapolation of the experimental data to zero titanium content represents the most valid value for nitrogen diffusion in chromium metal.

Table V. Comparison of Diffusion Data of Other Investigators

Method	Q, cal mole^{-1}	D_0, cm^2 sec^{-1}	Temperature Range, °C	Reference
Internal friction	20,500	3.5×10^{-6}	135 to 175	13
Internal friction and Elastic aftereffect	24,300	3.0×10^{-4}	50 to 175	12
Resistivity	25,700	*	140 to 200	14
Nitrogen profile	23,300	1.8×10^{-3}	1056 to 1233	11

*No value determined by this method.

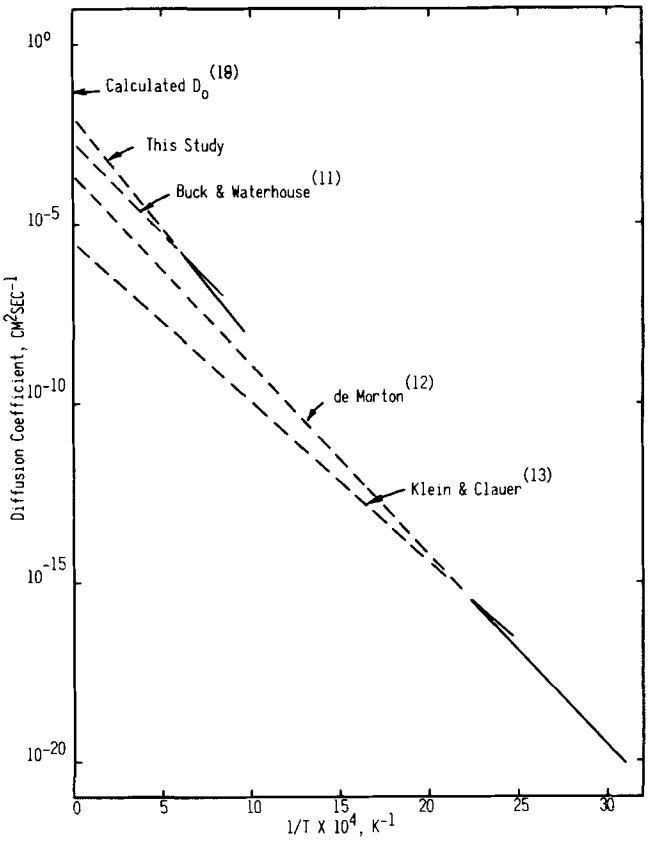

Fig. 8—Comparison of diffusion coefficients for nitrogen in chromium over a wide temperature range from different investigations.

SUMMARY

When titanium is added to chromium and these alloys are isothermally exposed to nitrogen, an outer scale of Cr_2N and an internal-nitride zone of fine TiN particles

grow parabolically. The latter zone thickness is controlled by nitrogen diffusion through the matrix, and it is possible to determine diffusion coefficients. Increasing titanium decreases activation energy and the preexponential constants for volume diffusion and Cr_2N scale growth. Individual D and k_p values are increased at lower temperatures over what would be expected from a linear extrapolation of higher temperature data. The TiN particles formed in various size distributions, and hardness measurements indicated maxima which decreased with higher temperatures and shorter times in a manner consistent with precipitation hardening.

ACKNOWLEDGMENT

The authors express their gratitude to the National Science Foundation for providing financial support of this research through a graduate traineeship to one of the authors (JLA) while seeking an advanced degree at the University of Denver.

REFERENCES

1. W. C. Hagel: *Trans. ASM,* 1963, vol. 56, p. 583.
2. A. U. Seybolt and D. H. Haman: *Trans. TMS-AIME,* 1964, vol. 230, p. 1294.
3. F. Henderson, S. T. Quaass, and H. C. Wain: *J. Inst. Metals,* 1954, vol. 83, p. 126.
4. N. E. Ryan and S. T. M. Johnstone: *J. Less-Common Metals,* 1965, vol. 8, p. 159.
5. C. Wagner: *Z. Elektrochem.,* 1959, vol. 63, p. 772.
6. F. Maak: *Z. Metallk.,* 1961, vol. 52, p. 545.
7. K. Schwerdtfeger: *Trans. TMS-AIME,* 1967, vol. 239, p. 1432.
8. Y. Adda and J. Philibert: *La Diffusion Dans Les Solides,* Presses Universitaines De France, Paris, 1966.
9. J. L. Meijering and M. L. Dreuyvesteyn: *Philips Res. Rep. no. 2,* pp. 81-102 and 260-280, 1942.
10. V. I. Arkharov, V. N. Konev, and A. Z. Menshikov: *Phys. Metal Metallogr.,* 1959, vol. 7, p. 58.
11. R. H. Buck and R. B. Waterhouse: *J. Less-Common Metals,* 1964, vol. 6, p. 36.
12. M. E. de Morton: *J. Appl. Phys.,* 1962, vol. 33, p. 2768.
13. M. J. Klein and A. H. Clauer: *Trans. TMS-AIME,* 1965, vol. 233, p. 1771.
14. C. W. Weaver: *Acta Met.,* 1962, vol. 10, p. 1151.
15. C. Wert and C. Zener: *Phys. Rev.,* 1949, vol. 76, p. 1169.
16. I. I. Spivak: *Phys. Metal Metallogr.,* 1966, vol. 22, p. 52.
17. D. I. Bolef and J. S. DeKlerk: *Phys. Rev.,* 1963, vol. 129, p. 1063.
18. C. Zener: *Imperfections in Nearly Perfect Crystals,* W. Schockley, ed., p. 289, J. Wiley, New York, 1952.
19. P. G. Shewmon: *Diffusion in Solids,* p. 64, McGraw-Hill, New York, 1963.